BioCore
Exploring Scientific Community

International Journal of Nanotechnology in Medicine & Engineering

Research Article
ISSN 2474-8811

The Effects of Nitrogen Ion Bombardment on Morphological Features of Synthesized Multilayer Graphene by LPCVD Method

R. Alipour*, A. Jafari, M. Ghoranneviss

Plasma Physics Research Center, Science and Research Branch, Islamic Azad University, Tehran, Iran

Abstract

Multilayer graphene films were synthesized on copper foil by means of low pressure chemical vapor deposition (LPCVD) and characterized using Raman spectroscopy. The Scanning Electron Microscopy (SEM), Atomic Force Microscopy (AFM) and the Mountains Map Premium 7.2 (64-bit version) software are used for investigation the effects of nitrogen ion bombardment on the morphological features of synthesized graphene film's surfaces. In this study, the analysis of the Minkowski functionals, the motifs, the depth histograms, the statistical parameters and the peak count histograms of the nanostructure surface of samples were implemented. These results are useful for better understanding of the characteristics and structures of synthesized graphene films.

Keywords: Graphene, LPCVD, Nitrogen Ion Bombardment, Morphological Properties

Corresponding author: **R. Alipour**

Plasma Physics Research Center, Science and Research Branch, Islamic Azad University, Tehran, Iran.

Email: alipour_r@ymail.com

Citation: R. Alipour et al (2018), The Effects of Nitrogen Ion Bombardment on Morphological Features of Synthesized Multilayer Graphene by LPCVD Method. Int J Nano Med & Eng. 3:1, 01-10

Received: December 20, 2017,

Accepted: December 30, 2017,

Published: January 29, 2018

Introduction

Graphene has received much attention recently in the scientific community because of its distinct properties and potential in nano-electronic applications. Many reports have been made on graphene's very high electrical conductivity at room temperature [1, 2] and its potential use as next-generation transistors [3], nano-sensors [4], transparent electrodes [5], and many other applications. Graphene can also be produced by chemical reduction of graphite oxide [6], high temperature annealing of single crystal SiC and mechanical exfoliation from highly ordered paralytics graphite. The most promising, inexpensive and readily accessible approach for deposition of reasonably high quality graphene is chemical vapor deposition (CVD) onto transition metal substrates such as Ni, Pd, Ru, Ir or Cu [6–10]. Experimental observed graphene has a lot of defects due to imperfect cutting. It is well-known that defect is ubiquitous in graphene and its effect on the structure and physical property has been studied extensively. Beyond chemical approaches [11], it was realized that defects created by ion irradiation also induce new functionalities [12, 13], or ways to form new nanostructures [14, 15]. The ion beam bombardment has been successfully used to improve the structural and corrosion resistance properties of material surfaces.

It has been demonstrated that ion irradiation, especially when combined with heat treatment, can also have beneficial effects on nanostructure materials. Experiments carried out for the technologically important carbon nanomaterials, such as nanotubes and graphene, showed that their atomic structure and morphology can be changed in a controllable manner by irradiation. When an energetic particle (ion or electron) penetrates a solid, it collides with the nuclei and the electrons of the target, so that the projectile energy is transferred to the target atoms. Although the low-energy (eV) incoming ions are quickly neutralized by capturing electrons from the target, in what follows, the incoming ion or atom is always referred to as "ion" to differentiate between the projectile and recoil atoms. If the target recoil atom acquires kinetic energy enough to leave its position in the atomic network, various atomic-scale defects may appear in the target. Many of the point defects, e.g., vacancy-interstitial pairs, disappear immediately after the impact, but some defects may remain in the system or form more complicated defect structures. However, little attention was paid to achieving the doping effect and functionalization on the surfaces of graphene by low energy ion beam bombardment. Among the numerous potential dopants, nitrogen is considered to be an excellent candidate for the doping of carbon materials. This is because of its comparable atomic size and the presence of five valence electrons available to form strong

valence bonds with carbon atoms, which would produce N-doping graphene[16–18].

Based on this case, in this work, a low energy N ion beam was used to bombard the graphene surface using an ion implantation set up. Our purpose was to study the morphological change in graphene surface due to nitrogen ion bombardment. Firstly, multilayer graphene film was grown by low pressure chemical vapor deposition and then the effects of the nitrogen ion bombardment were studied using Raman spectroscopy, scanning electron microscopy (SEM) and atomic force microscopy (AFM).

Experimental Technique

Our experiments contained two parts. Firstly multilayer graphene synthesis was carried out using a LPCVD set up. A schematic of the LPCVD set-up used for the synthesis of graphene is shown in Fig. 1. The 1 × 1 cm2 Copper foil with (001) crystallographic orientation was used as a substrate. The thickness of Cu substrate was 100 μm. Before growth, the Cu substrates were cleaned by flotation in acetone and put into the ultrasonic device for 15 min. This process is repeated by using of alcohol and deionized water, respectively. Then the substrates were loaded in the LPCVD quartz tube.

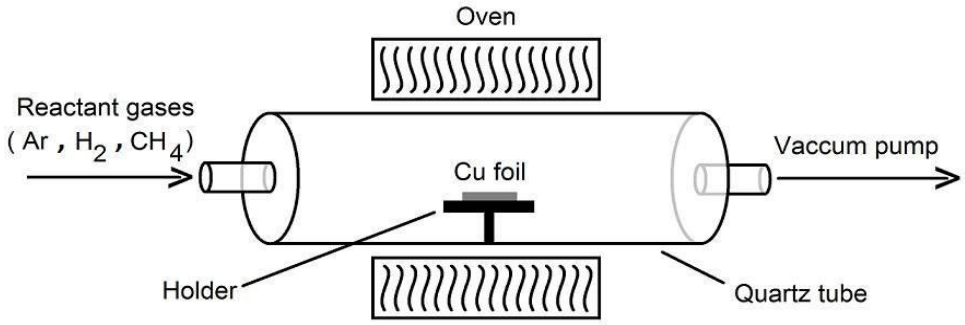

Fig. 1: Schematic of LPCVD set-up

The experimental instrument consists of a quartz tube, an LPCVD chamber, heating system, vacuum pump and channel gas flowing systems. The Cu foil was heated up to 950 oC and maintained for 60 min in an Ar atmosphere without changing the Ar flow rate and pressure in order to activate grain growth and improve the crystallinity of the Cu substrate. The growth was started in a mixture of gases (H2 : CH4 = 70% : 30%) while the growth pressure was 1 Torr.Subsequently, the substrate was heated up to the desired temperature. After 10 min, reaction time, the furnace was cooled to room temperature, under Ar flow for carbon segregation and graphene formation. It is worth noting that in the LPCVD process, initial heating of the substrate is required to allow for the formation of Cu grains on which graphene domains can nucleate and grow.

Nitrogen ion bombardment was performed on graphene samples with the approximate areas of 1 cm2 with 30 keV energy and 1 × 10 18 ion cm-2 dose at room temperature .The angle between the implanted ions and graphene surface was 900. The current density of ion beam in the experiment was 120 (μAcm-2) and during the implantation, the sample temperature was kept at 100 °C. During the nitrogen bombardment, the base N2 gas pressure in the chamber was 10 -6 Torr. The incident ions lose their energy due to collisions with the carbon atoms and come to rest in the near-surface region. A schematic of the ion bombardment system used for the graphene nitrogen implantation is shown in Fig. 2. Depending on ion mass, the ions used in materials science for irradiation and implantation are traditionally splitin to two categories: light and heavy ions. Normally H, He, and sometimes Li ions are referred to as "light," while ions of other chemical elements are treated as "heavy". So, here we used heavy ion in order to ion bombardment. Another important parameter is the irradiation dose.

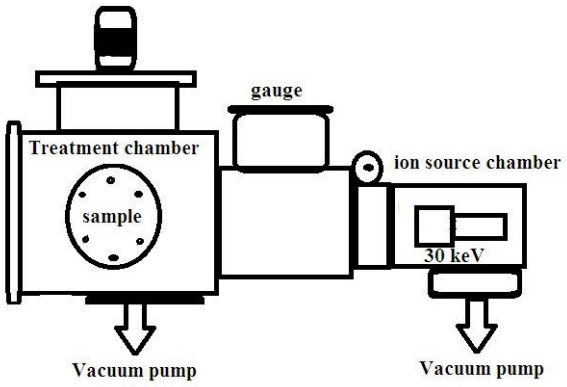

Fig. 2: Schematic of nitrogen ion bombardment system

One can define "low dose" as the dose corresponding to the situation when the defected regions created by different ions do not overlap. Conversely, "high dose" irradiation means that many ions hit the same microscopic area of interest. Therefore nitrogen ions with 1×10^{18} ion cm^{-2} dose effect as a high dose.

Results and discussion

Due to a well-controlled structure, graphene can be an ideal system for studying the effects of ion irradiation on solid targets in various regimes corresponding to the nuclear and electronic stopping. Indeed, contrary to bulk solids, every displacement of atoms from a suspended monoatomic graphene under ion irradiation should give rise to the formation of a defect, as the displaced atoms will be sputtered away, so that recombination of vacancy-interstitial pairs is not possible. The presence of defects was confirmed by Raman spectroscopy. In Fig. 3 the Raman spectra of multilayer graphene films, before and after the N ion bombardment are compared. Three main peaks are assigned in the Raman spectrum: a D band (~1350 cm^{-1}), G band (~1585 cm^{-1}) and 2D band (~2684 cm^{-1}).

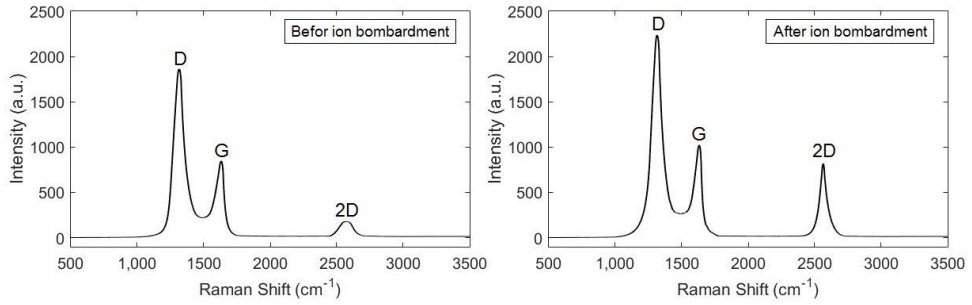

Fig. 3: Raman spectra of deposited and nitrogen ion bombarded multilayer graphene film

The G peak is known to be associated with the doubly degenerate phonon mode at the Brillouin zone center, indicating sp2 carbon networks in the sample [21]. In Raman spectra of graphene and graphene-like material the 2D band is the second order of zone-boundary phonons originates from a second-order Raman process and it is used to determine the thickness of graphene and graphene layers [22]. The presence of defects gives rise to a D peak, which initially is forbidden in non-defective graphene as a result of Raman selection rules. This peak corresponds to the so-called disorder induced D band, which is activated by a double resonance effect by defects, such as vacancies, crystalline boundaries, edge defect and so on [23, 24].

The deposited graphene on copper foils that used in this work consists of highly defective of graphene, as can be deduced from the high ID/IG ratio. In the Raman spectra of graphene and other sp2 carbon samples containing defects, several additional symmetry breaking features are found. The feature with the highest intensity is usually the D band. The D band is associated with near-K point phonons and the intensity of the D peak also shows the quality and defect in lattice structure of samples [25, 26]. The results of Raman analysis are shown in Table 1.

Sample	I_D	I_G	I 2D
Before nitrogen ion bombard	1852.32	874.59	188.27
After nitrogen ion bombard	2246.71	1014.66	834.12

Table 1: The results of Raman analysis

As can be seen in Table 1, the intensity of the D peak increased after nitrogen ion bombardment. It means that after nitrogen ion bombardment, the defect in lattice structure of synthesized graphene samples and the quality of them increased and decreased, respectively.

The number of graphene layers can be calculated by using of the intensity ratio of the 2D peak to the G peak. As mentioned above, the 2D band in Raman spectra is a second order of two phonon process. It exhibits an unusually strong frequency dependence on the excitation laser due to a double resonance process which links the phonon wave vector to the electronic band structure. This feature can be used for the determination of the number of graphene layers. While a graphene monolayer can be fitted by a single Lorentzian peak, a bi-layer requires four Lorentzians, which are related to the four possible double resonance scattering processes when only one is possible for the monolayer. When the number of layers increases, the number of double resonance processes also increases and the spectral shape converges to that of graphite, where only two peaks are observed. The full width at half-maximum of the 2D band is found to be a quantitative guide to distinguish the layer number (single layer to five layers) of FLG. The splitting of the electronic band structure in FLG is responsible for the stepwise broadening of 2D bands according to the theoretical model of double resonance, whiles it is known that

the distance between graphene layers is about 0.335 nm in graphite lattice. Low intensity and broad 2D peak in the Raman spectrum in our experiment indicates that this sample has a lot of layers. Also, Table 1 shows that the ratio of I2D to IG for all samples are less than 2 and the multilayer graphene are grown on the Cu substrates.

A major effect of N ion beam bombardment is to increase the clustering of the sp2 phase, which is indicated by the D peak intensity increasing. We refer to ID/IG as the ratio of peak heights. No significant shifts of any of the peaks were observed in Fig. 3. A significant difference in the intensity of D bands can be observed after bombardment. The D band arises from the limitations in the graphene domain size, induced by grain boundaries or imperfections, such as substitution of N atoms or other impurities. When nitrogen ion collides with nuclei of the carbon atom, it can be scattered significantly and transfer its energy to the carbon atom in graphene lattice (nuclear stopping). In the hard collision, lattice atom can get enough energy to break free from the lattice binding energy, which causes lattice disorder and damage crystal structure. When projected ion hits the nucleus, it constituents nuclear stopping. When the projected ion enter into substrate, it gets aligned with the gap between the host atoms, and they travel a large distance before finally coming to rest (ion channeling).

Comparing ID/IG of pure graphene before and after N ion bombardment shows a higher ID/IG after bombardment and a higher sp2 fraction [23]. It clearly shows that the ID/IG intensity ratio depends on the number of irradiated layers, i.e. it is higher by decreasing the number of layers. It is known that the production of defects into a single graphene layer due to ion irradiation is influenced strongly by the presence of one or more underlying planes [27]. This is plausible since in the case of a multi-layer system the same ion, in its collision cascade, induces defects in a very large number of planes around the same spatial region. These defects are free to evolve and interact each other during the cascade quenching [28]. Particularly for partial/oblique collisions the atoms could be captured between the layers, allowing them to migrate and heal vacant sites. XPS analysis was performed to investigate chemical states and N atomic concentrations of the surfaces. To probe nitrogen atoms in the N-doped graphene structure, we carried out XPS measurements. While elemental analysis gives the amount of nitrogen doped into the graphene lattice, the nature of nitrogen can only be confirmed by XPS. The bond-dissociation energy of C-C bond is around 3.5 eV while the energy of nitrogen ions was 30Kev, therefore nitrogen ions have enough energy to break C-C bonds and formation of N-C bonds. The XPS results are shown in Fig. 4 which confirm the presence of N in the sample. Three peaks appearing at 285.13, 399.68 and 532.68 eV can be assigned to C1s, N1s and O1s respectively.

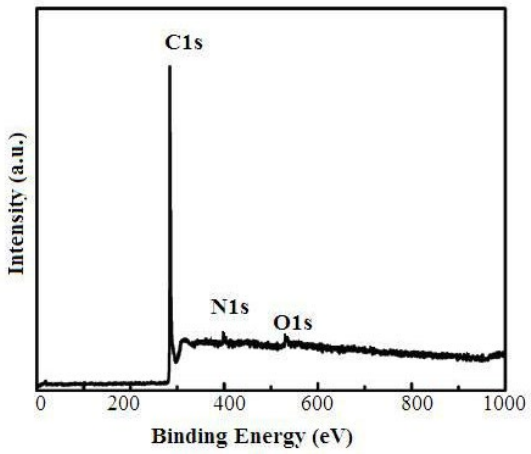

Fig. 4: X-ray photoelectron spectrum (XPS) of the graphene film after nitrogen bombarded

The appearance of a weak O1s peak in XPS spectra comes from the presence of residual gas in gas mixing. The emergence of the peak at 399.68 eV means that N ion beam bombardment causes the formation of new N-containing groups. These refer to the nitrogen atoms that are located in the graphene lattice replacing carbon atoms. Three kinds of C–N bonding configurations are obtained when doping nitrogen into the graphene lattice: pyridinic N, pyrrolic N, and graphitic N. Our XPS results show that N ions have been incorporated into the graphene hexagonal structure, as reflected by the pyrrolic-like XPS N1s peak at 399.68 eV [29, 30, 32]. Pyrrolic N in graphene lattice indicate that the graphene sample before nitrogen bombardment certainly has lattice defect like vacancy.

Fig. 5 shows SEM images of graphene grown on Cu foils before and after nitrogen ion bombardment. Nucleation of graphene domains with an average domain size of ~5 μm is observed that is full covered on the Cu surface. This domain morphology is similar to diamond reported previously [33]. Also the grain boundary is sharply defined before the ion bombardment. In addition, no wrinkles can be observed in any images, implying that vacuum can promote the segregation of dissolved carbon from the Cu foil.

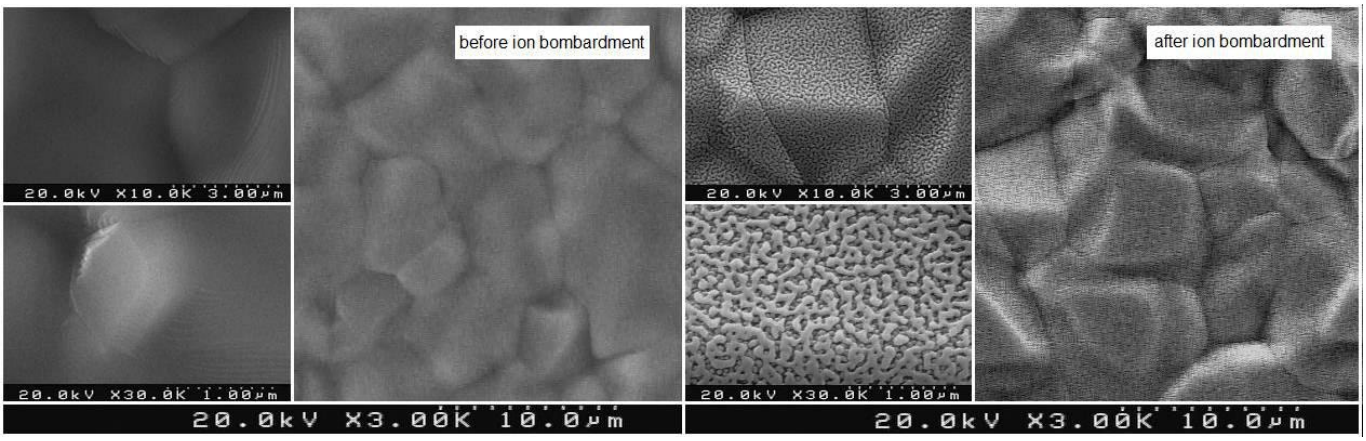

Fig.5: SEM image of the synthesized graphene films on Cu foil before and after nitrogen ion bombardment.

In general, some significant change in the surface morphology can be observed after N ion bombardment. To prove this result, a bigger magnification is used to observe the change in morphology after N ion beam bombardment, so just some holes could be seen on the graphene surface after ion bombardment. The release of surface atoms by the impact of an energetic nitrogen ion is called "sputtering". Also swift heavy ions can sputter materials due to electronic excitations. An effect frequently associated with high energy sputtering is "cratering", i.e. the formation of a surface depletion in the region of ion impact. Due to a highly complex interaction with the material's elastic and plastic properties, craters often coexist with nearby hillocks, and sometimes hillocks have even been observed alone. This description confirms the effect of nitrogen ion bombardment from AFM results. The 2D and 3D AFM images of Cu substrate and synthesized graphene films before and after N ion bombardment are shows in Figs. 6 and 7, respectively.

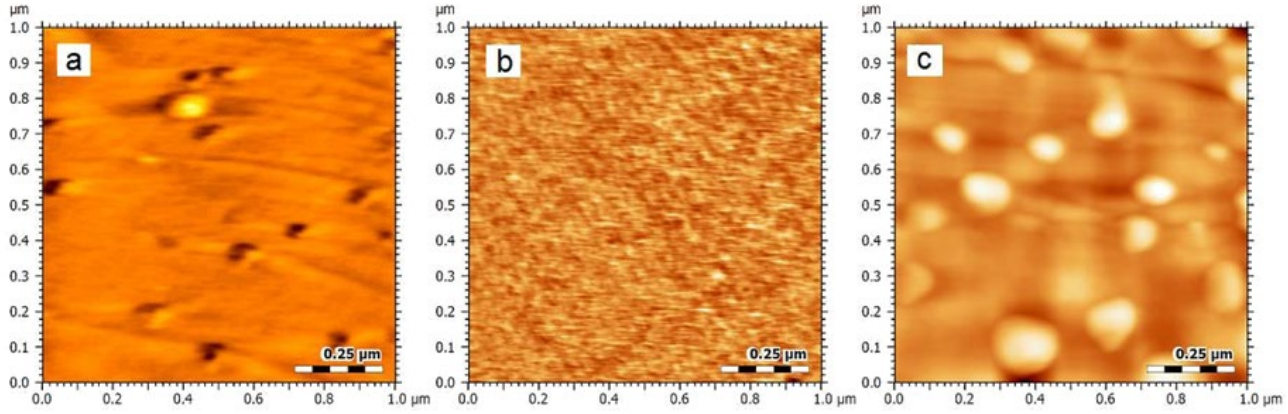

Fig. 6: 2D AFM images of the surface of (a) the Cu foil and the synthesized graphene film samples (b) before nitrogen ion bombardment and (c) after nitrogen ion bombardment.

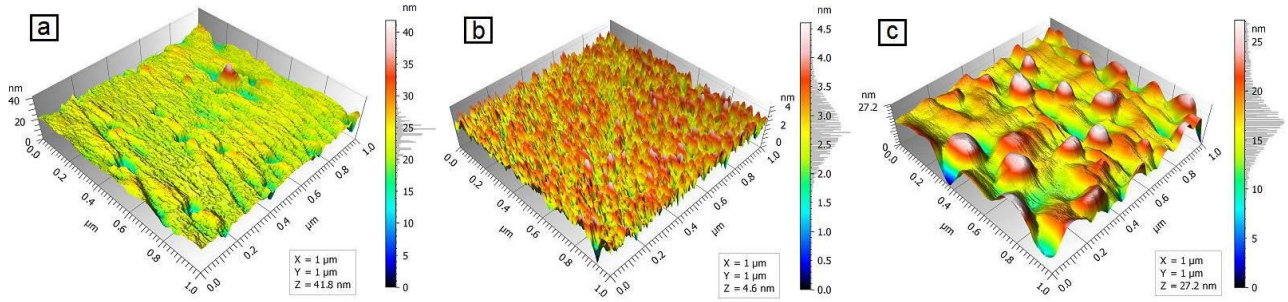

Fig. 7: 3D AFM images of the surface of (a) the Cu foil and the synthesized graphene film samples (b) before nitrogen ion bombardment and (c) after nitrogen ion bombardment.

It can be seen from these images that the many fine peaks with sharp hillock-like features in graphene surface before ion bombardment deform to higher peaks after ion bombardment; also the flat and smooth area can be seen in some zones due to the ion bombardment. These effects and changes can be explained by the collision between the nitrogen ions and carbon atoms of graphene surface. Such collisions cause displacement of atoms from their equilibrium positions in the graphene network. This is the main mechanism for slow ions (low ion energy regime). Fig. 8 Shows motifs (or texture cell) detection of specifications on surfaces and analysis by watersheds algorithms, according to ISO 25178 [34]. The watershed segmentation is a mathematical morphological tool for image segmentation, based on geodesic operators, which can automatically segment images into a series of closed segmentation regions [35].

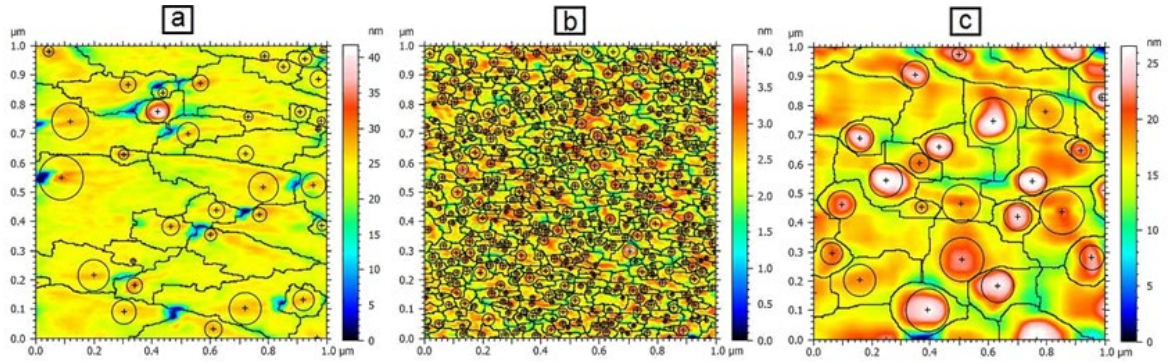

Fig. 8: The motifs images of (a) the Cu foil and the synthesized graphene films on Cu foil (b) before nitrogen ion bombardment and (c) after nitrogen ion bombardment.

The motifs results show that the synthesized graphene layers contains of the circular grains or oblong grains. In other words, the shape of grown particles can be determined by using of these results. In this research, to calculate the motifs analysis, the Mountains Map Premium software (64-bit version)[36] is used. The parameters for the motifs analysis (surface) of the 3-D surface roughness, according with ISO 25178-2: 2012 are shown in Table 2.

Table 2: The motifs analysis according to ISO 25178 for samples of the Cu foil and the synthesized graphene films before and after nitrogen ion bombardment.

Parameters	Cu foil	Before nitrogen ion bombardment	After nitrogen ion bombardment
Number of motifs	38	503	36
Mean Height [nm]	4.152272	0.452681	5.463543
Mean area [μm^2]	0.026472	0.001998	0.027942
Mean perimeter [µm]	0.810305	0.199328	0.777745
Mean of mean diameter [µm]	0.145298	0.041901	0.165390
Mean of min diameter / Mean of max diameter [µm] / [µm]	0.091207 / 0.266671	0.026228 / 0.070703	0.112512 / 0.261457
Mean of equivalent diameter [µm]	0.157448	0.044295	0.174262
Mean aspect ratio	2.964604	2.993414	2.537145
Mean roundness	0.418524	0.431883	0.469779
Mean compactness	0.636486	0.648685	0.676576
Mean sphere radius [µm]	0.067305	0.018279	0.201634

The mean aspect ratio parameter can be obtained by measuring the ratio of the maximum diameter to the minimum diameter. If the value is close to 1, the form of the grain is close to disk. If the value is higher than 1, the grain is oblong. The mean roundness parameter shows the ratio of the average value between the area of the grain and the area of the disk. If this value is close to 1, the form of the grain is close to disk and if this value is less than 0.5, the grain is oblong. Also, the mean compactness can be calculated by measuring the average ratio of the equivalent diameter and the maximum diameter. If this value is close to 1, the form of the grain is close to disk. If this value is close to 0.5, the grain is oblong. All these parameters show that the synthesized graphene layers are composed of the oblong grains. The most important of the statistical parameters of 3D surface roughness of graphene film samples, according to ISO 25178-2: 2012, are shown in Table 3.

Table 3: The most important of statistical parameters for the Cu foil substrate and the synthesized graphene film samples before and after nitrogen ion bombardment according to ISO 25178.

Statistical parameters	Symbol	Cu foil	Before nitrogen ion bombardment	After nitrogen ion bombardment
Height Parameters				
Root mean square height	Sq [nm]	3.124704908	0.4420792719	3.235667186
RMS roughness	Rq [nm]	150	0.8182	7.685
Average roughness	Ra [nm]	97.3	0.6451	4.101
Skewness	Ssk	-2.062866772	0.1082727236	0.4467816368
Kurtosis	Sku	13.52796346	3.092624279	4.149066486
Maximum peak height	Sp [nm]	18.17272069	1.79645894	9.934060985
Maximum pit height	Sv [nm]	23.62727931	2.80354106	17.26593901
Maximum height	Sz [nm]	41.8	4.6	27.2
Spatial Parameters				
Auto-correlation length	Sal [μm]	0.02994359469	0.01236635	0.06150187486
Texture-aspect ratio	Str	0.5644017634	0.23029624	0.8658960785
Feature Parameters				
Density of peaks	Spd [1/μm²]	23	644	4
Mean dale area	Sda [μm²]	0.013248333	0.00123359	0.03145371
Mean hill area	Sha [μm²]	0.022987838	0.00114949	0.033502506
Mean dale volume	Sdv [μm³]	5.970957e-006	6.7754521e-008	1.013090e-005
Mean hill volume	Shv [μm³]	1.2112677e005	6.8897554e-008	2.799238e-005

The results show that the RMS and the average roughness of graphene samples are increased after nitrogen ion bombardment. Skewness limit is the parameter to indicating the symmetry of the height distribution. The negative values of this parameter represents a surface with valleys while the positive values demonstrates a surface with peaks. It can be seen in the Table 3 that these parameter for the graphene sample before nitrogen ion bombardment is close to zero. It means that the number of valleys and peaks on the surface of synthesized graphene before nitrogen ion bombardment are almost equally while the number of peaks compared to the number of valleys are increased after nitrogen ion bombardment. The surface flatness of samples can be measured by the kurtosis (Sku) parameter. The surface of samples is spiky if this parameter be greater than 3 and for bumpy surfaces, the Sku is less than 3. For random surfaces, the kurtosis parameter must be approximately equal to 3. The results in Table 3 represent that the surface of graphene samples before nitrogen ion bombardment is random while it become spiky after nitrogen ion bombardment. The texture aspect ratio parameter show that the surface is isotropic (have the same characteristics in all directions) or anisotropic (have an oriented or periodical structure). For isotropic surfaces, this parameter is close to 1 and for anisotropic surfaces, this parameter is close to 0. In can be seen in Table 3 that the surface of graphene samples before nitrogen ion bombardment is anisotropic while it become isotropic after nitrogen ion bombardment. The averaged power spectral density of samples are shown in Fig. 9. The horizontal axis is graduated in wavelengths, and the vertical axis displays the amplitude to a power of 2 [35].

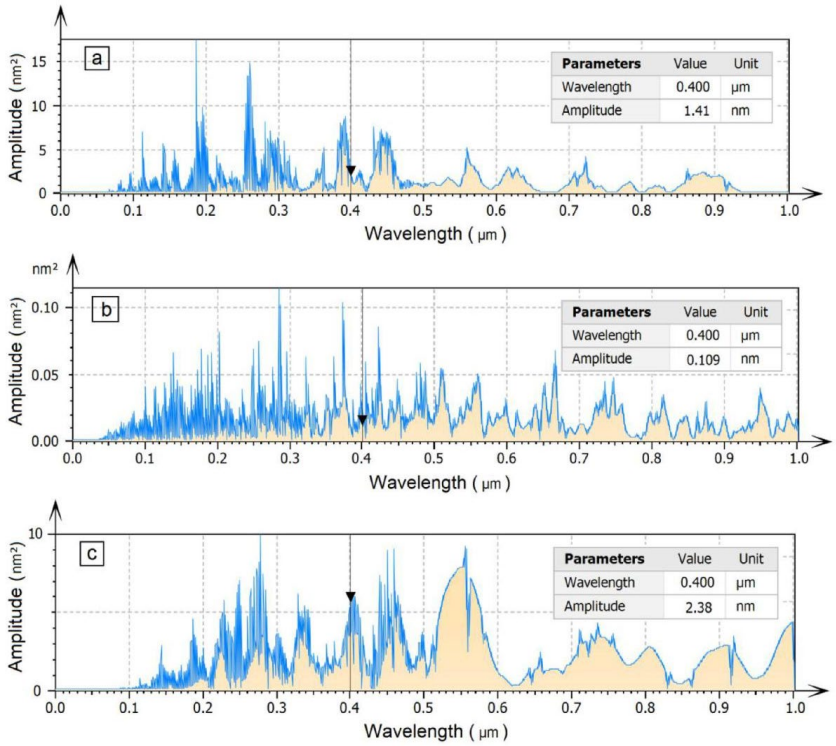

Fig. 9: The averaged power spectral density of (a) the Cu foil and the synthesized graphene film samples (b) before nitrogen ion bombardment and (c) after nitrogen ion bombardment.

The averaged power spectral density was estimated from the matrix of values and gives the topography of the measured samples, for the scanning area of the nanostructure surfaces of samples. This parameter shows that at which frequencies variations are strong and at which frequencies variations are weak [39]. It can be seen in Fig. 9 that the amplitude of variations are increased significantly, after nitrogen ion bombardment.

Conclusion

Low energy N ion beam was used to bombard the surface of multilayer graphene film prepared with LPCVD method on Cu foil with an energy of 30 keV at room temperature. In order to investigate the effect of the nitrogen bombardment on structural changes of graphene, Raman spectroscopy, Scanning electron microscopy and atomic force microscopy are used. Raman spectroscopy showed a significant difference in the intensity of D band after nitrogen bombardment. This means the N ion bombardment induced imperfections and N impurity in the graphene atomic structure. This causes the D band to increase due to defects in the carbon materials. SEM images show in significant change in the surface morphology of the graphene sample before and after the bombardment which confirms that samples are not damaged after N bombardment. The motifs analysis show that the synthesized graphene layers are composed of the oblong grains. The results show that the RMS and the average roughness of graphene samples are increased after nitrogen ion bombardment. Skewness limit shows that the number of valleys and peaks on the surface of synthesized graphene before nitrogen ion bombardment are almost equally while the number of peaks are increased after nitrogen ion bombardment. The kurtosis parameter represents that the surface of graphene samples before nitrogen ion bombardment is random while it become spiky after nitrogen ion bombardment. The texture aspect ratio parameter show that the surface of graphene samples before nitrogen ion bombardment is anisotropic while it become isotropic after nitrogen ion bombardment.

Reference

1. Novoselov K S, Geim A K, Morozov S V, Jiang D, Zhang Y, Dubonos S V, Grigorieva I V and Firsov A A 2004 Science 306 666

2. Lin Y M, Jenkins K A, Garcia A V, Small J P, Farmer D B and Avouris P 2008 Nano Lett. 9 422

3. Wang X, Zhi L and Mullen K 2008 Nano Lett. 8 323

4. Schedin F, Geim A K, Morozov S V, Hill E W, Blake P, Katsnelson M I and Novoselov K S 2007 Nat. mater. 6 652

5. Bae S, Kim H, Lee Y and Xu X 2010 Nat. Nanotechnol. 5 574

6. Bourlinos A B, Gournis D, Petridis D, Szabo T, Szeri A and Dekany I 2003 Langmuir 19 6050

7. Kraus J, Bocklein S, Reichelt R, Gunther S, Santos B, Mentes T O and Locatelli A 2013 Carbon 64 377

8. Zhang J, Hu P, Wang X and Wang Z 2012 Chem. Phys. Lett. 536 123

9. Kumar A, Voevodin A A, Zemlyanov D, Zakharov D N and Fisher T S 2012 Carbon 50 1546

10. Sarno M, Cirillo C, Piscitelli R and Ciambelli P 2013 J. Mol. Catal. A: Chem. 366 303

11. Hern S C, Boutilier M S H, Idrobo J C, Song Y, Kong J, Laoui T, Atieh M and Karnik R 2014 Nano Lett. 14 1234

12. Ugeda M M, Brihuega I, Guinea F and Rodriguez J M G 2010 Phys. Rev. Lett. 104 096804

13. Ugeda M M, Torre D F, Brihuega I, Pou P, Galera A J M, Perez R and Rodriguez J M G 2011 Phys. Rev. Lett. 107 116803

14. Standop S, Lehtinen O, Herbig C, Malandrakis G L, Craes F, Kotakoski J, Michely T, Krasheninnikov A and Busse C 2013 Nano Lett. 13 1948

15. Ahlgren E H, Hamalainen S K, Lehtinen O, Liljeroth P and Kotakoski J 2013 Phys. Rev. B 88 155419

16. Cun H, Iannuzzi M, Hemmi A, Osterwalder J and Greber T 2014 ACS Nano 8 7423

17. Zhao W, Hofert O, Gotterbarm K, Zhu J F, Papp C and Steinruck H P 2012 J. Phys. Chem. C 116 5062

18. Koch R J, Weser M, Zhao W, Vines F, Gotterbarm K and Kozlov S M 2012 Phys. Rev. B

86 075401

19. Adler R J and Taylor J E 2007 Random fields and geometry (New York, USA: Springer)

20. Gwyddion Software User Guide, Version 2.4, Available: www.gwyddion.net (2015)

21. Ferrari A, Meyer J, Scardaci V, Casiraghi C, Lazzeri M, Mauri F, Piscanec S, Jiang D, Novoselov K, Roth S and Geim A 2006 Phys. Rev. Lett. 97 187401

22. Graf D, Molitor F, Ensslin K, Stampfer C, Jungen A, Hierold C and Wirtz L 2007 Nano Lett. 7 238

23. Ferrari A C and Robertson J 2000 Phys. Rev. B 61 14095

24. Venezuela P, Lazzeri M and Mauri F 2011 Phys. Rev. B 84 035433

25. Jafari A, Ghoranneviss M, Gholami M and Mostahsan N 2015 Int. Nano Lett. 5 199

26. Beams R, Cancado L G and Novotny L 2015 J. Phys. Condens. Matter. 27 083002

27. Compagnini G, Giannazzo F, Sonde S, Raineri V and Rimini E 2009 Carbon 47 3201

28. Ewels C P, Telling R H, El-Barbary A A, Heggie M I and Briddon P R 2003 Phys. Rev. Lett. 91 025505

29. Su Y, Jiang H, Zhu Y, Yang X, Shen J, Zou W, Chen J and Li Ch 2014 J. Mater. Chem. A 2 7281

30. Xu Y, Mo Y, Tian J, Wang P, Yu H and Yu J 2016 Appl. Catal. B 181 810

31. Nardecchia S, Carriazo D, Ferrer M L, Gutierreza M C and Monte F D 2013 Chem. Soc. Rev. 42 794

32. Scardamaglia M, Aleman B, Amati M, Ewels C, Pochet P, Reckinger N, Colomer J F, Skaltsas T, Tagmatarchis N, Snyders R, Gregoratti L and Bittencourt C 2014 Carbon 73 371

33. Song M, Ameen S and Akhtar M Sh 2013 Mater. Res. Bull. 48 4538

34. ISO 25178-2: 2012, Geometrical Product Specifications (GPS) - Surface Texture: Areal - part 2: Terms, Definitions and Surface Texture Parameters, Available: www.iso.org

35. Alipour R, Meshkani S and Ghoranneviss M 2015 Eur. Phys. J. Appl. Phys. 71 10302

36. Mountains Map Premium (64-bit version) software, available: www.digitalsurf.fr

37. Johnson K L 1985 Contact Mechanics (Cambridge University Press) p 407

38. Stachowiak G W and Batchelor A W 2001 Engineering tribology (Boston, Butterworth-Heinemann) p 450

39. Selvaraj H, Chmaj G and Zydek D 2015 Progress in Systems Engineering (Springer International Publishing) p 280